A generalized pressure impulse framework for wave slamming problems

Daniel Vig Muff[1,2], Morten Christensen[1], Henrik Bredmose[2] and Fabio Pierella[2]
[1]LICengineering—Part of the NIRAS Group, Esbjerg, Denmark
[2]Department of Wind Energy, Technical University of Denmark, Kgs. Lyngby, Denmark
dvm@liceng.dk

1. INTRODUCTION

Impulsive hydrodynamic loads, or wave slamming, pose critical challenges to offshore and coastal structures, occurring during short-duration, high-pressure impacts such as breaking waves or hull entries. Accurate prediction is essential for designing resilient systems like wind turbine foundations and ship hulls. Existing methods range from high-fidelity CFD, which is accurate but computationally expensive, to simplified analytical models based on classical works by von Kármán and Wagner [1, 2], which rely on restrictive assumptions. Pressure impulse theory [3] offers an efficient alternative by reducing the problem to solving Laplace's equation for the pressure impulse field, capturing dominant inertial effects during impact. However, current formulations are largely analytical and limited to simple geometries.

This paper introduces a generalized FEM framework for pressure impulse theory, enabling accurate modeling of complex three-dimensional structures and boundary conditions while maintaining efficiency. The method is verified against an analytical solution [4] and its versatility is demonstrated for a wave impact on a floating box.

2 PRESSURE IMPULSE THEORY

Let $P : \Omega \to \mathbb{R}$ be the pressure impulse defined by

$$P(\mathbf{x}) = \int_{t_0}^{t_0+\tau} p(\mathbf{x}, t)\,\mathrm{d}t, \quad \mathbf{x} \in \Omega, \tag{1}$$

with $\Omega \subset \mathbb{R}^3$ representing the fluid domain, t_0 the initial time, and τ the impulse duration. The instantaneous pressure p is governed by the Navier-Stokes equations. For a slamming impact over a characteristically small time interval τ, viscosity, convective acceleration, and body forces are negligible compared to the unsteady inertia term. Assuming the fluid is incompressible, the governing equation simplifies to

$$\rho\frac{\partial \mathbf{u}}{\partial t} = -\nabla p, \tag{2}$$

where ρ is the fluid density and $\mathbf{u}(\mathbf{x}, t) \in \mathbb{R}^3$ is the velocity field.

Integrating over the interval $[t_0, t_0+\tau]$ yields the impulse-momentum relationship $\rho\Delta\mathbf{u} = -\nabla P$, where $\Delta\mathbf{u} = \mathbf{u}(t_0 + \tau) - \mathbf{u}(t_0)$ is the change in velocity over the impact duration. Taking the divergence of both sides and invoking the incompressibility constraint ($\nabla\cdot\mathbf{u} = 0$), we find that the pressure impulse satisfies the Laplace equation

$$\nabla^2 P(\mathbf{x}) = 0, \quad \mathbf{x} \in \Omega. \tag{3}$$

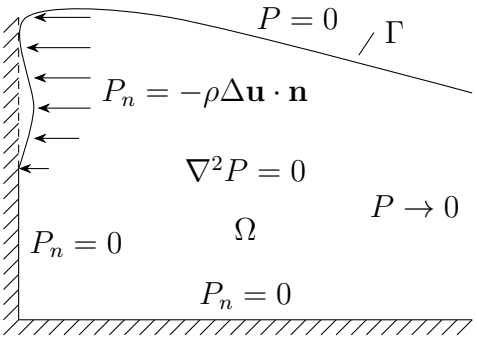

Figure 1: Sketch of the pressure impulse fluid domain Ω and boundary Γ, with boundary conditions representing an overturning wave impacting a vertical structure.

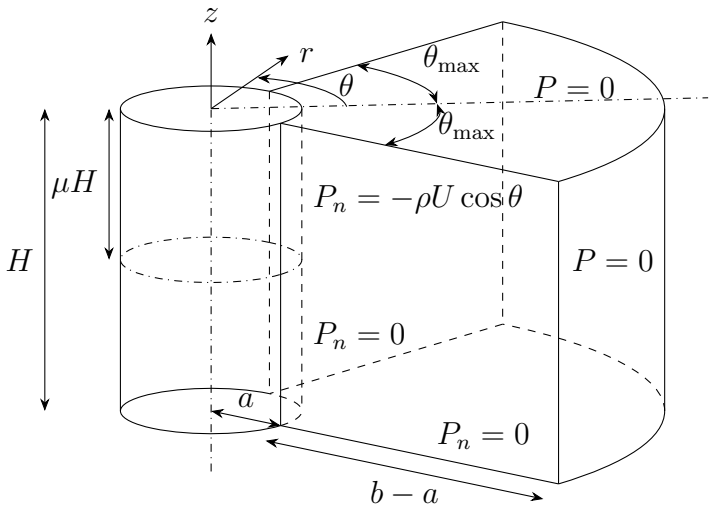

Figure 2: Sketch of the wedge-shaped impact on a vertical cylinder including boundary conditions.

Let $\Gamma := \partial\Omega$ denote the boundary of the domain Ω, see Figure 1, the boundary conditions can then be prescribed as

$$P(\mathbf{x}) = \bar{P}(\mathbf{x}), \quad \mathbf{x} \in \Gamma_{\mathrm{D}} \subset \Gamma \text{ (Dirichlet)} \tag{4a}$$

$$P_n(\mathbf{x}) = \bar{P}_n(\mathbf{x}), \quad \mathbf{x} \in \Gamma_{\mathrm{N}} \subset \Gamma \text{ (Neumann)} \tag{4b}$$

with $P_n := \partial P/\partial n$ meaning the derivative along the normal vector $\mathbf{n}$ on Γ, the bar denoting specified quantities, taking either zero or non-zero values, and $\Gamma = \Gamma_{\mathrm{D}} \cup \Gamma_{\mathrm{N}}$ and $\Gamma_{\mathrm{D}} \cap \Gamma_{\mathrm{N}} = \varnothing$.

3 NUMERICAL FRAMEWORK

To implement the numerical scheme in a FEM setting, we recast the strong form of the governing equation (3) into its variational (weak) form, relaxing differentiability requirements by seeking an integral solution over the domain Ω. We introduce the test function $v \in H_0^1(\Omega)$, which ensures square-integrability of the pressure impulse P and its first derivatives while satisfying Dirichlet boundary condition $v = 0$ on Γ_{D}.

Multiplying the governing equation $\nabla^2 P = 0$ by the test function and integrating over the fluid domain yields

$$\int_\Omega v \nabla^2 P \,\mathrm{d}\Omega = 0. \tag{5}$$

Using Green's first identity, the second-order derivative is reduced to a product of first-order derivatives. This "integration by parts" procedure transfers one level of differentiation from the trial function P to the test function v

$$\int_\Omega \nabla v \cdot \nabla P \,\mathrm{d}\Omega - \int_\Gamma v P_n \,\mathrm{d}\Gamma = 0. \tag{6}$$

As v vanishes on Γ_{D}, the boundary integral is only evaluated over the Neumann boundary Γ_{N}. Substituting the gradient $P_n = \bar{P}_n$ from Equation (4b), we arrive at the final weak form

$$\int_\Omega \nabla v \cdot \nabla P \,\mathrm{d}\Omega = \int_{\Gamma_{\mathrm{N}}} v \bar{P}_n \,\mathrm{d}\Gamma. \tag{7}$$

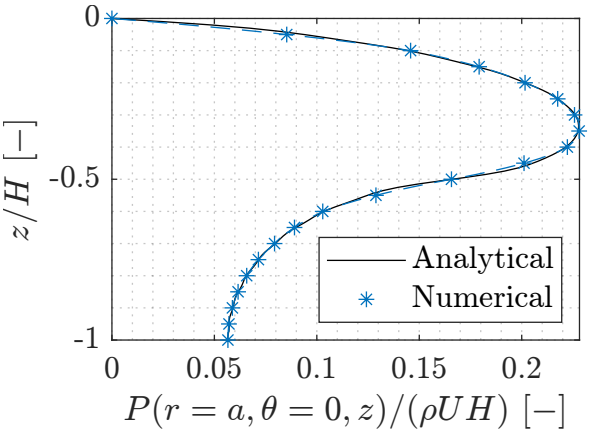

Figure 3: Pressure impulse along the center of the cylinder face ($r = a, \theta = 0, z$).

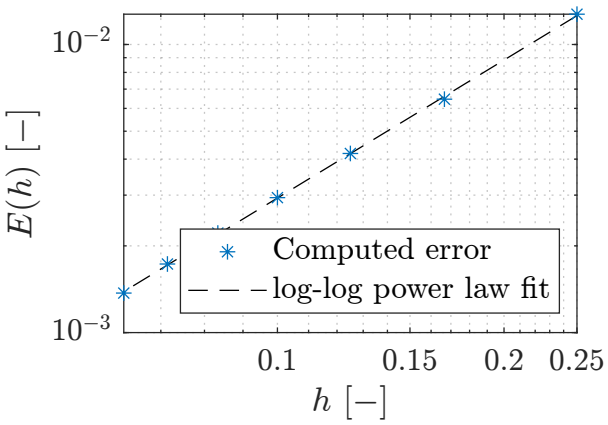

Figure 4: Convergence of error $E(h)$ in log–log space.

3.2 Discretization

To solve the weak form numerically, the domain Ω is discretized into a mesh of N nodes and non-overlapping elements. We approximate the continuous solution $P(\mathbf{x})$ and the test function $v(\mathbf{x})$ using a Galerkin approach

$$P(\mathbf{x}) \approx \sum_{i=1}^{N} \phi_i(\mathbf{x}) P_i, \quad v(\mathbf{x}) \approx \sum_{j=1}^{N} \phi_j(\mathbf{x}) v_j, \tag{8}$$

where ϕ_i are basis (shape) functions with local support; meaning they are nonzero only on elements connected to node i. This locality ensures the resulting system matrix is sparse. Substituting these approximations into the weak form (7) and requiring the residual to vanish for all admissible v_j yields the linear algebraic system

$$\mathbf{KP} = \mathbf{f}, \tag{9}$$

where $\mathbf{P} = [P_i] \in \mathbb{R}^N$ is the vector of the nodal pressure impulse. The global system matrix $\mathbf{K} = [K_{ij}] \in \mathbb{R}^{N \times N}$ and contributions from the Neumann boundary conditions $\mathbf{f} = [f_i] \in \mathbb{R}^N$ are defined by

$$K_{ij} = \int_{\Omega} \nabla \phi_i \cdot \nabla \phi_j \, \mathrm{d}\Omega, \quad f_i = \int_{\Gamma_{\mathrm{N}}} \phi_i \bar{P}_n \, \mathrm{d}\Gamma. \tag{10}$$

In practice, the integrals for K_{ij} and f_i are evaluated numerically over individual elements. The resulting local element matrices are then assembled into the global system (9) using the mesh connectivity. The system is solved for $\mathbf{P}$ using either direct or iterative linear solvers.

4 VERIFICATION OF IMPLEMENTATION

The numerical framework is verified against the analytical solution for cylindrical wedge impact [4], chosen to evaluate the interaction between high-order element discretization and curved geometric boundaries. The domain Ω and its boundary conditions are defined in Figure 2, where $r \in [a, b]$, $\theta \in [-\theta_{\max}, \theta_{\max}]$, and $z \in [-H, 0]$.

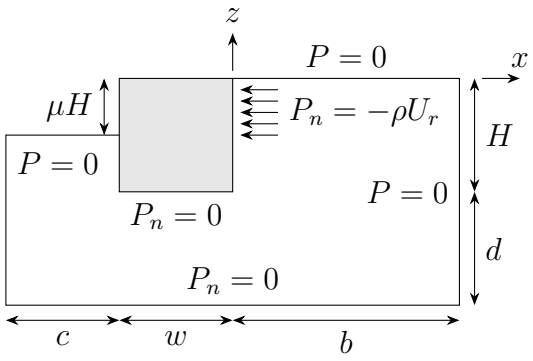

Figure 5: Sketch of the impact on a floating box including boundary conditions.

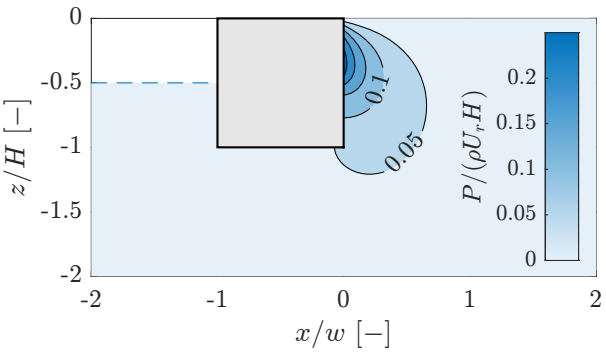

Figure 6: Pressure impulse contour.

For this example, we have used cylinder radius $a = 1$ m, outer boundary $b = 3$ m, and height $H = 1$ m. The impact is characterized by a wedge angle $\theta_{\max} = \pi/4$ and a relative impact height $\mu = 1/2$. Physical properties include fluid density $\rho = 1025$ kg/m^3 and impact velocity $U = 11$ m/s.

Numerical discretization utilizes quadratic isoparametric hexahedral elements. A $10 \times 10 \times 10$ mesh is employed; while adaptive refinement could optimize computational cost in high-gradient regions, a non-adaptive mesh is sufficient for this comparison.

Figure 3 demonstrates excellent agreement between the numerical implementation and the analytical solution for the chosen discretization, confirming the accuracy of the proposed framework. The convergence of the root-mean-squared error E, measured along the vertical profile at $(r = a, \theta = 0)$, is illustrated in Figure 4. The observed trend confirms the accuracy and consistency of the implementation as relative mesh size h decreases.

To demonstrate the versatility of the proposed numerical framework, we consider the simplified wave impact on a floating rectangular box, see Figure 5. The pressure impulse is depicted in Figure 6 for $H = d = 1$ m, $w = c = b/2 = 1$ m, $\mu = 1/2$, $\rho = 1025$ kg/m^3, and a relative impact velocity $U_r = 3$ m/s. Notably, we observe that the impact results in a pressure on the bottom of the box, introducing a vertical component to the forcing. The presented example demonstrates the application of the framework for problems beyond the verification case. Future work will focus on extending the application to a three-dimensional truncated vertical cylinder and validating the results against experimental data.

REFERENCES

[1] von Kármán, T. 1929. The impact on seaplane floats during landing. Tech. rep., National Advisory Committee for Aeronautics.

[2] Wagner, H. 1932. *Über Stoß- und Gleitvorgänge an der Oberfläche von Flüssigkeiten.* Zeitschrift für Angewandte Mathematik und Mechanik 12(4), 193–215.

[3] Cooker, M. J., and Peregrine, D. H. 1995. *Pressure-impulse theory for liquid impact problems. Journal of Fluid Mechanics 297*, 193–214.

[4] Ghadirian, A., and Bredmose, H. 2019. *Pressure impulse theory for a slamming wave on a vertical circular cylinder. Journal of Fluid Mechanics 867*, R1.